A vibration technique for nondestructively assessing the integrity of structures

Kitami Institute of Technology　○Student Member　Sherif Beskhyroun
Kitami Institute of Technology　Fellow　Toshiyuki Oshima
Kitami Institute of Technology　Member　Shuichi Mikami
Kitami Institute of Technology　Member　Tomoyuki Yamazaki

1. Introduction

The ability to monitor the condition of a structure to detect damage at early stages is of significant interest to many structure owners. This paper provides an overview of a method to detect, locate, and characterize damage in structural systems by examining changes in measured vibration response. The basic idea behind this technology is that the dynamic response is a function of the physical properties of the structure. Therefore, changes in the physical properties will cause detectable changes in the dynamic response. Various spectral functions are used to estimate the dynamic response of the structure, and then the changes in these functions due to the presence of damage are estimated at all frequency components on the measurement range instead of using modal amplitude, which can be called operational mode shapes. The first and most important objective of the damage identification algorithm presented here is to ascertain with confidence if damage is present or not. Thus, at each frequency component, the damage will be detected with more confidence if it could be detected using all different spectral functions. The applicability of this methodology is evaluated using the experimental data measured from a railway steel bridge.

2. Theoretical description

2.1 Spectral Analysis

Before the damage identification algorithm is presented several terms related to spectral analysis are defined.

For a continuous time series, $x(t)$, defined on the interval from 0 to T, the Fourier Spectrum (Fourier Transform), $X(f)$, is defined as

$$X(f) = \int_0^T x(t)e^{-i2\pi ft}dt \tag{1}$$

where $i = \sqrt{-1}$, and f = cyclic frequency (Hz).
This function is complex. Its magnitude is typically plotted in engineering units (EU), such as m/s^2 or g, versus frequency. The power spectrum is defined as

$$\left|X(f)\right|^2 = X(f)X^*(f) \tag{2}$$

where * denotes a complex conjugate. The Power Spectral Density (PSD), $G_{xx}(f)$ is defined as

$$G_{xx}(f) = \frac{2}{T}E\left[\left|X(f)\right|^2\right] \tag{3}$$

where $E[\ ]$ indicates an ensemble average for a specific f over n samples of $X(f)$. The Cross Spectral Density (CSD), $G_{xy}(f)$, relating two time histories, $x(t)$ and $y(t)$ is defined as

$$G_{xy}(f) = \frac{2}{T}E\left[X^*(f)Y(f)\right]. \tag{4}$$

For a linear system Transfer Function Estimate (TFE) which relates an input, $X(f)$, to a response, $Y(f)$, is defined as

$$T_{xy}(f) = \frac{Y(f)}{X(f)} = \frac{G_{xy}(f)}{G_{xx}(f)}. \tag{5}$$

The coherence function $H_{xy}(f)$, relating two time histories, $x(t)$ and $y(t)$ is defined as

$$H_{xy}(f) = \frac{\left|G_{xy}(f)\right|^2}{G_{xx}(f)G_{yy}(f)}. \tag{6}$$

The phase angle $A_{xy}(f)$, between two time histories $x(t)$ and $y(t)$ can be computed from the real and imaginary values of G_{xy} as

$$A_{xy}(f) = \tan^{-1}\left[imag(G_{xy}(f))/real(G_{xy}(f))\right]. \tag{7}$$

2.2 Damage detection algorithm[1)]

Let $G_i(f)$ denote the spectral function magnitude measured at channel number i at frequency value f. The absolute difference in spectral function magnitude before and after damage can then be defined as

$$D_i(f) = \left|G_i(f) - G_i^*(f)\right| \tag{8}$$

where $G_i(f)$ and $G_i^*(f)$ represent spectral function magnitude for the undamaged and damaged structures respectively. The excitation forces used for the undamaged and damaged structure must have the same amplitude and waveform in order to ensure that the changes in spectral function magnitude data are mainly due to damage. When the change in spectral function magnitude is measured at different frequencies on the measurement range from f_1 to f_m, a matrix [**D**] can be formulated as follows

$$\mathbf{D} = \begin{bmatrix} D_1(f_1) & D_2(f_1) & .... & D_n(f_1) \\ D_1(f_2) & D_2(f_2) & .... & D_n(f_2) \\ . & . & .... & . \\ . & . & .... & . \\ . & . & .... & . \\ D_1(f_m) & D_2(f_m) & .... & D_n(f_m) \end{bmatrix} \tag{9}$$

where n represents the number of measuring points. In matrix [**D**], every row represents the changes in spectral function magnitude at different measuring channels but at the same frequency value. The summation of spectral function magnitude changes over different frequencies can be used as the indicator of damage occurrence and the increase in damage. In other words, the first damage indicator is calculated from the sum of columns of matrix [**D**] as

$$\mathbf{TD} = \left\{\sum_f D_1(f) \quad \sum_f D_2(f) \quad . \quad . \quad . \quad \sum_f D_n(f)\right\}. \tag{10}$$

However, the total change in spectral function magnitude was found to be a weak indicator of damage localization. A statistical decision making procedure is employed to determine the location of damage. The first step in this procedure is the selection of the maximum change in spectral function magnitude at each frequency value (the maximum value in each row of matrix [**D**]) and discarding all other changes in spectral function magnitude measured at other nodes. For example in matrix [**D**], if $D_3(f_1)$ is the maximum value in the first row then this value will be used as $M_3(f_1)$

and other values in this row will be discarded. The same process is applied to the different rows in matrix [**D**] to formulate the matrix of maximum changes of spectral function magnitude at different frequencies, [**M**]

$$\mathbf{M}=\begin{bmatrix} 0 & 0 & M_3(f_1) & 0 & .... & 0 \\ 0 & M_2(f_2) & 0 & 0 & .... & 0 \\ 0 & 0 & 0 & M_4(f_3) & .... & 0 \\ . & . & . & . & .... & . \\ . & . & . & . & .... & . \\ 0 & 0 & M_3(f_m) & 0 & .... & 0 \end{bmatrix}. \qquad (11)$$

The total of maximum changes in spectral function magnitude is calculated from the sum of the columns of matrix [**M**]

$$\mathbf{TM}=\left\{\sum_f M_1(f) \quad \sum_f M_2(f) \quad . \quad . \quad . \quad \sum_f M_n(f)\right\}. \qquad (12)$$

In order to monitor the frequency of damage detection at any node, a new matrix [**C**] is formulated. The matrix consists of 0's at the undamaged locations and 1's at the damaged locations. For example in the matrix [**C**], we put a value of 1 corresponding to the locations of $M_3(f_1)$, $M_2(f_2)$ and so on, as shown in the following expression

$$\mathbf{C}=\begin{bmatrix} 0 & 0 & 1 & 0 & .... & 0 \\ 0 & 1 & 0 & 0 & .... & 0 \\ 0 & 0 & 0 & 1 & .... & 0 \\ . & . & . & . & .... & . \\ . & . & . & . & .... & . \\ 0 & 0 & 1 & 0 & .... & 0 \end{bmatrix}. \qquad (13)$$

In matrix [**C**], at each frequency line (each row) the location of damage is represented by 1. Therefore, the total number of times of detecting the damage (total number of frequency lines at which damage is detected) at different nodes is calculated from the sum of the columns of matrix [**C**] as

$$\mathbf{TC}=\left\{\sum_f C_1(f) \quad \sum_f C_2(f) \quad . \quad . \quad . \quad \sum_f C_n(f)\right\}. \qquad (14)$$

The damage localization indicator is defined as the scalar product of {**TM**} and {**TC**} as shown in the following expression

$$\mathbf{DI}=\{TM(1)\times TC(1) \quad TM(2)\times TC(2) \quad . \quad . \quad . \quad TM(n)\times TC(n)\} \qquad (15)$$

3. Railway steel bridge: description and experimental setup

The experimental work in this research was performed on a railway steel bridge that is no longer in service. The bridge consists of two steel plate girders and two steel stringers support the train rails. Loads from the stringers are transferred to the plate girders by floor beams located at various intervals. The bridge dimensions and layout are shown in Fig. 1. The multi-layer piezoelectric actuator is used for local excitation. The actuator force amplitude is 200 N. Although this force amplitude is very small compared to shaker forces or ambient vibrations, it was enough to excite the web of the main girder at the position of the farthest accelerometer. Two actuators are used for exciting the web of the main girder in the horizontal direction. The actuators are located at the upper part on the web of the main girder (Fig. 1). The excitation forces used for the undamaged and damaged structure are sweep, equal in amplitude and have the same vibration waveform but the excitation force does not need to be measured. Eight accelerometers were used to measure the acceleration response in the horizontal direction. One accelerometer is mounted at the geometrical center of gravity of each panel of the main girder, as shown in Fig. 1. All of the connections of different elements of the bridge are riveted and no damage could be introduced to these connections. Only two angles (look like stiffeners) are bolted to the web of main girder. Therefore, it was decided to remove the bolts one by one from the right angle to introduce damage to the main girder.

4. Damage Identification results

4.1 Damage identification using different spectral functions

PSD is calculated at each measuring channel from the acceleration time history data using MATLAB Standard and MATLAB Signal Processing Toolbox. Hanning window of size 256 is applied to the time signals to minimize leakage. In this technique, the signal (acceleration data) is divided into overlapping sections (50% overlap) of the specified window length (256) and windows each section using the Hanning window function. In such case, the PSD can be measured at 129 frequency lines in the frequency range of 1-800 Hz (frequency step = 800*2/256). In the proposed damage identification algorithm the magnitude of the power spectral function can be used in any frequency range (from f_1 to f_m). In order to avoid the problem of identifying the frequency range in which PSD has to be used in the proposed algorithm, it was decided to use PSD in the total measured range (1-800 Hz). As clearly indicated in Fig. 1, channel number 5 is the closest sensor to the damage location. Damage localization indicator is used to identify the damage location as shown in Fig. 2 (a). Damage localization indicator determined the damage location at channel 5 accurately with some false positive readings at other channels. These false positive readings are assumed to be due to the presence of noise and measurement errors in the measured data and also can be due to the accuracy of the damage identification algorithm. This accuracy is considerably high since releasing one bolt from one stiffener is considered a very small damage compared to the size of the test structure. Moreover, the number of false positive readings decreased significantly after removing more bolts from the stiffener; the results are not shown here due to the limited size of the paper. Fig. 2 (b) shows the frequency values at which damage location is detected at channel 5. This figure is obtained from the fifth column in matrix [**M**] (Eq. 11) and explains how the damage is detected at channel 5 using PSD data at each frequency line in the frequency range of 1-800 Hz. For example, damage location is determined most accurately when PSD is measured in the frequency range of 720-800 Hz. In this range, damage is detected at channel 5 at almost every frequency line and the changes in PSD are higher. It should be noted that the frequency ranges (or lines) which gives accurate results are randomly distributed in the total measurement range (from 1-800 Hz). It was also noticed that the frequency range that gives accurate results in certain damage case changes when the damage level increases at the same location or when the damage location changes. Therefore, it was decided to use PSD (and other spectral functions) data in the total measured frequency range. The number of bars in Fig. 2 (b) (equals 45) represents the number of times of detecting damage at channel 5, out of 129 frequency lines used for measuring the PSD data. This value can be estimated using Eq. (14). The estimated value at the damage location will be used to compare the performance of each spectral function when it is used in the proposed algorithm.

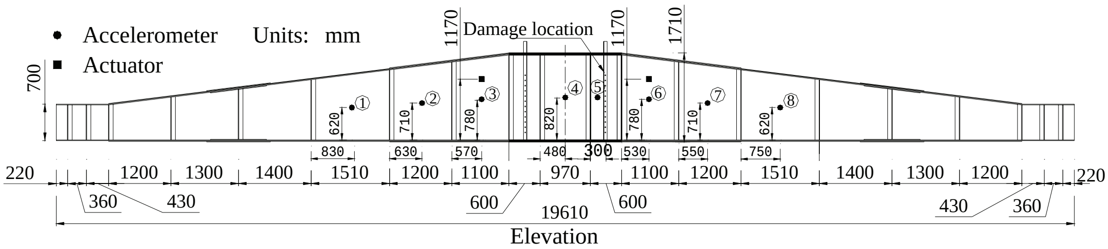

Fig. 1 Bridge layout and main dimensions

CSD is estimated from the acceleration time history measured at each channel relative to the acceleration time history at channel 3. Using channel 3 as a reference yielded the most accurate results for CSD and the following spectral functions. Therefore, it was decided to use the obtained results, using this channel as a reference, for comparison with PSD function. The influence of changing the location of the reference channel on the accuracy of identifying damage location will be discussed later in this chapter. The same procedures that were used in PSD will also be used here and for the other spectral functions presented in this study to allow for better comparison of these functions. Fig. 3 (a) shows more accurate results in identifying damage location at channel 5 than using PSD. However, the difference in accuracy is very small and changing the reference channel sometimes produces less accurate results than PSD function. Fig. 3 (b) shows that the frequency ranges (or lines) that give accurate results in this case are not always the same ranges that gave accurate results in case of using PSD. This explores one important fact that the frequency range that gives false positive readings, when using certain spectral function, does not always contain high noise or measurement errors since the same range may give accurate results when another spectral function is used and vice versa. This is also another reason to use the magnitude of the spectral function in the total measured frequency range rather than looking for the best frequency range that will give the most accurate results. The number of times of detecting damage at channels 5 equal 46 increasing by one from the case of using PSD. Similar results and observations were obtained when TFE, PHASE and COHERENCE data were used in the proposed algorithm, as shown in Figs. 4 through 6. All functions yielded accurate results in identifying the damage location.

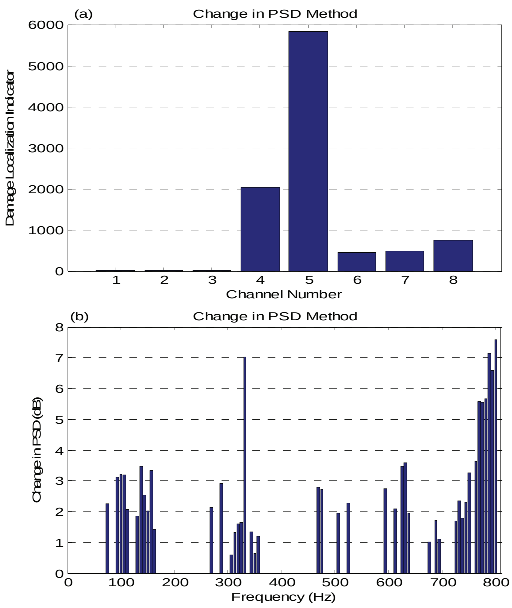

Fig. 2 Damage identification results using PSD

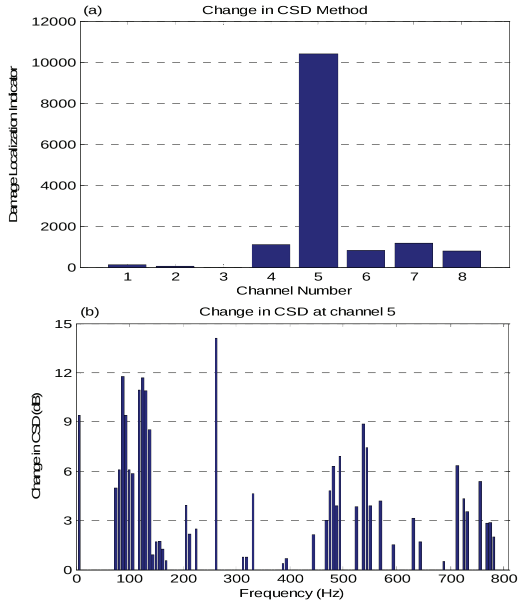

Fig. 3 Damage identification results using CSD

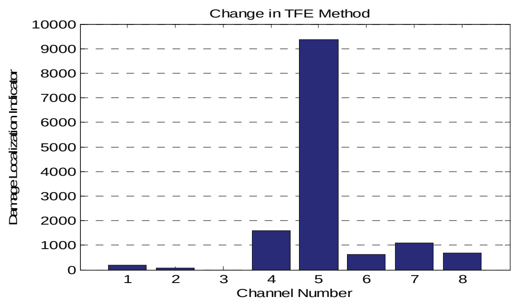

Fig. 4 Damage identification results using TFE

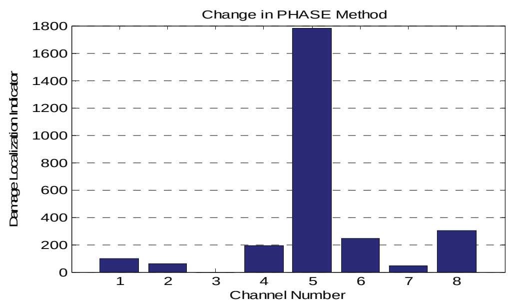

Fig. 5 Damage identification results using PHASE

4.2 The confidence of detecting damage using different spectral functions

Table 1 shows the number of times of detecting the damage at channel 5 for different damage levels using different spectral functions data. All functions yielded similar results in case of removing the first bolt. When the second bolt was removed, the number of times of detecting the damage increased significantly using PSD compared to using other spectral functions. The increase in the number of times

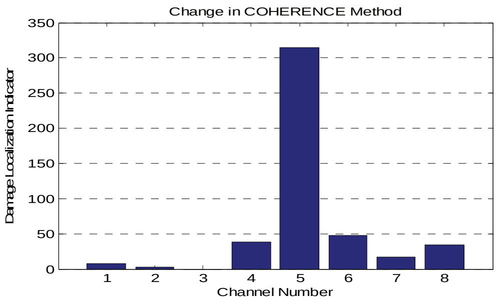

Fig. 6 Damage identification results using COHERENCE

Table 1: Number of times of detecting the damage

	1 Bolt	2 Bolts	3 Bolts	4 Bolts
PSD	45	80	76	79
CSD	47	45	57	56
TFE	44	48	56	60
PHASE	45	55	55	57
COHERENCE	48	39	43	42

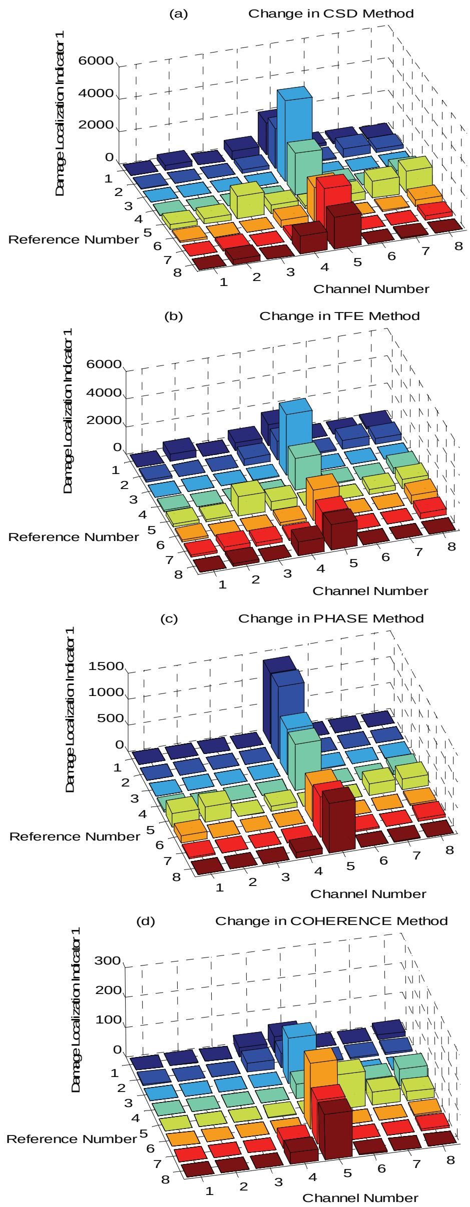

Fig. 7 Effect of changing the reference channel location

of detecting the damage at certain location increases the confidence of detecting the damage at this location and decreases the possibility of false positive readings. After removing the third and the fourth bolts, the use of PSD data yielded the most accurate results. Using COHERENCE data yielded the lowest number of times of detecting the damage in cases of removing 2, 3 and 4 bolts. It was noticed that the increase in damage level is not always associated with the increase in the number of times of detecting the damage using all spectral functions except TFE.

4.3 The influence of changing the location of reference channel

The influence of changing the location of the reference channel is examined by using each channel once as a reference for other channels. In order to reduce the effect of noise, another damage localization indicator is defined as follows: a value of one standard deviation of the elements in vector {**TM**} is subtracted from the vector {**TM**}. Any resulting negative values are discarded. The same procedure is applied to the vector {**TC**}. The new damage indicator (1) is obtained from the scalar product of the resulting vectors. Fig. 7 shows the obtained results of the different spectral functions. It is clearly indicated in this figure how the accuracy of locating the damage varies with the change of the location of the reference channel. For example, in case of using CSD using channel 3 as a references yielded the most accurate results while using channel 8 yielded the least accurate results. The accuracy of locating the damage did not change significantly in case of using PHASE data. Using the input force as a reference needs further investigation.

5. Conclusions

The application of a linear damage identification method using experimental modal data gathered from a railway steel bridge has been reported. Five different spectral functions were used to estimate the modal response of the structure. This study investigates the applicability of the proposed method to detect and locate small damage using the output response of the structure without the need to measure the input excitation force. The study also provides a direct comparison of various spectral functions that can be used to estimate the modal response. Damage could be detected and located at the nearest sensor location using all the spectral functions. However, using PSD function has shown the most accurate results in detecting damage with more confidence. All spectral functions presented here have the advantage of being estimated from the response of the structure without the need to measure the excitation force. This feature is useful when ambient vibration is used as an excitation source for continuous health monitoring of structures where it is difficult to measure the ambient excitation forces. Another observation from this study is that the accuracy of locating the damage, when CSD, TFE, and COHERENCE functions are used, depends on the location of the reference channel. The PHASE function has shown consistent results regardless of the reference channel location. In this study, it was observed that the best frequency range in which the magnitude of the spectral function should be used in the proposed algorithm depends not only on the damage location or type but also on the type of the spectral function. Therefore, it is recommended to use the spectral function magnitude in the total measurement range as it is extremely difficult to determine the best frequency range in which the spectral function data should be measured.

References

1) Beskhyroun S., Oshima T., Mikami S., Tsubota Y., Structural damage identification algorithm based on changes in power spectral density, *Journal of Applied Mechanics, JSCE*, Vol.8, pp. 73-84, 2005.